

Simulating galactic outflows in ultrafaint dwarf galaxies

D. Romano¹, F. Calura¹, A. D’Ercole¹, and G. C. Few²

¹ Istituto Nazionale di Astrofisica – Osservatorio di Astrofisica e Scienza dello Spazio di Bologna, via Gobetti 93/3, 40129 Bologna, Italy, e-mail: donatella.romano@inaf.it

² E. A. Milne Centre for Astrophysics, University of Hull, Cottingham Road, Kingston Upon Hull HU6 7RX, UK

Abstract. In the past fifteen years, a new class of galaxy has been discovered that is made of faint, old, scarcely evolved stellar systems –the so-called ultrafaint dwarf galaxies (UFDs). High-resolution, three dimensional hydrodynamical simulations are a powerful tool to investigate the nature, origin, and evolution of UFDs, but they are extremely expensive in terms of computational time. We took advantage of high performance computing (HPC) resources provided by CINECA through the MoU INAF-CINECA and started a project devoted to the study of UFDs. This report updates and extends a previous one.

1. Introduction

In the past fifteen years, the number of known Milky Way companions has increased apace. A new class of galaxy has been discovered that is made of extremely faint, dark-matter dominated, scarcely evolved stellar systems, which have been named ultrafaint dwarf galaxies (UFDs; see Simon 2019 for a review of discoveries and galaxy properties). Deep photometric observations of UFDs are best fit by ancient stellar populations (e.g. Brown et al. 2014); in some cases, deep images are consistent with a single-epoch, short burst of star formation (Okamoto et al. 2012).

All of this has impacted our understanding of the way the halo of our Galaxy came into being and moved the focus to studies aimed at establishing how star formation and chemical enrichment proceed in the smallest dark matter halos.

2. Background and motivation

Semi-analytical and pure chemical evolution models have been used first to follow the evolution of systems with structural properties resembling those of UFDs. By introducing simple heuristic (yet physically motivated) recipes to treat complex processes, such as accretion, cooling, star formation, and radiative feedback, these models have efficiently explored (in terms of computational cost) a wide range of parameter space (e.g. Salvadori & Ferrara 2009; Vincenzo et al. 2014; Romano et al. 2015). It has been concluded that star formation in UFDs was a very inefficient process, but no firm constraints could be put on the quenching mechanism(s), mainly because of the idealized treatment of the dynamical processes at play. The natural outcome is to turn to hydrodynamical simulations.

Overall, there are not that many hydrodynamical studies devoted to UFDs in the litera-

ture. Bland-Hawthorn et al. (2015) adopted the three-dimensional (3D) hydro-ionization code Fyris Alpha (Sutherland 2010) to track the response of adiabatic and cooling models, with clumpy or smooth gas distributions, to a single supernova (SN) explosion, occurring either at the center or off-center of isolated UFD-sized halos. In Webster et al. (2015), the same authors considered the effects of an extended star formation. Their main conclusion was that UFDs form in low-mass halos, rather than being the remnants of larger systems. Jeon et al. (2017) performed N-body/TreePM SPH simulations of relatively isolated systems outside the virial radius of a MW-like host halo (a choice that allows to minimize the computational cost by excluding processes such as tidal interactions and ram pressure stripping; see, however, Emerick et al. 2016). Jeon et al. suggested that the combined effect of reionization and SN feedback is responsible for quenching the star formation in UFDs. More recently, Corlies et al. (2018) used adaptive mesh refinement (AMR) cosmological simulations to study the formation and evolution of UFDs. Although they can recover some observational properties of Local Group UFDs, the theoretical stellar metallicity distributions are still too narrow and metal-rich.

3. High-resolution 3D simulations of SN explosions in UFDs

The HPC resources granted to the account INA17_C3B16 have been used to complete our fiducial set of high-resolution 3D simulations of SN feedback in the prototype UFD Boötes I. Overall, our project used more than 1e6 CPU hrs (see Table 1) and comprises adiabatic as well as cooling models. The simulation setup and results are briefly described in the remainder of this section; more details can be found in Romano et al. (2019).

4. Simulation setup

We run our simulations with a customized version of the AMR code RAMSES (Teyssier 2002). The initial configuration is designed to

Table 1. Total computational cost for the project described in this report. Our fiducial high-resolution adiabatic simulation to 30 Myr costs on the order of 300,000 CPU hrs, while the radiative simulation required 700,000 CPU hrs out to 20 Myr. About 200,000 CPU hrs were devoted to convergence and other tests.

Account	CPU hrs	Cluster
IsC22_BoSNex	50,000	EURORA, Galileo
IsC30_BoSNexII	200,000	Galileo
IsC39_BoSNex3	140,000	Galileo
INA17_C1B01	300,000	Marconi, Marconi KNL
INA17_C3B16	500,000	Marconi KNL

mimic the Boötes I UFD, and foresees a non-rotating distribution of gas and stars embedded in an isolated dark matter halo. The theoretical initial baryonic and dark masses are $M_{\text{gas}} = 6 \times 10^6 M_{\odot}$ and $M_{\text{DM}} = 3.5 \times 10^7 M_{\odot}$, respectively, and follow a Plummer (1911) and a Burkert (1995) density profile; the characteristic Plummer radius is about 200 pc, while the dark matter cut-off radius is about 1.2 kpc. The gas is assumed to follow a smooth, single-phase distribution reflecting that observed nowadays for long-lived stars in Boötes I. The dark matter component is modeled as a static external potential and added to the solution of the Poisson equation. Owing to the dark matter dominance, the self-gravity of the gas is neglected, for simplicity. Solving the hydrostatic equilibrium equation sets the initial pressure profile.

A population of coeval stars with mass $M_{\text{stars}} = 1 \times 10^5 M_{\odot}$ is set in place at the beginning of the simulation, i.e., we consider an instantaneous burst of star formation. This choice maximizes the effects of stellar feedback, since it leads to the highest synergy among the stellar-wind and SN-driven bubbles. A canonical stellar initial mass function (Kroupa 2001) is assumed. According to this choice, 650 stars end up as core-collapse SN progenitors with masses in excess of $8 M_{\odot}$. These stars are grouped in OB associations (hereinafter OBAs) 2 r_{OBA} wide, with r_{OBA} set to 4 pc for the high-resolution, fully converged

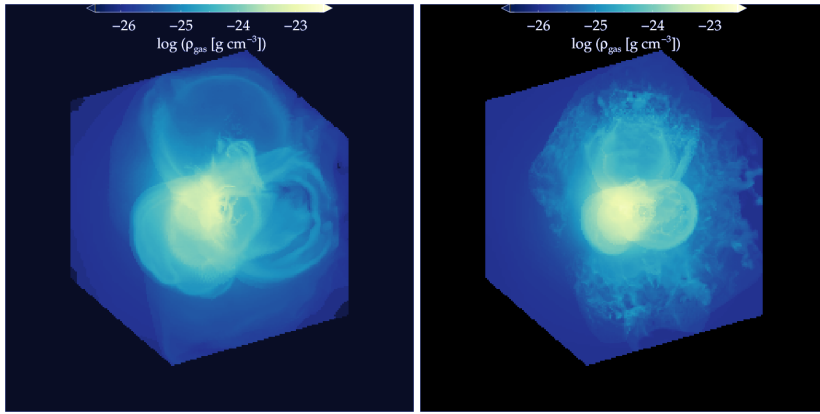


Fig. 1. 3D distribution of the gas in the simulation box at $t = 20$ Myr for the adiabatic (left-hand panel) and cooling (right-hand panel) high-resolution models. The box size is $(2 \text{ kpc})^3$, the minimum cell size is 0.95 pc.

simulations. Each OBA ejects mass and energy in its surroundings for 30 Myr (roughly corresponding to the lifetime of a $8 M_\odot$ star) through stellar winds and SN explosions, at a constant rate, following Leitherer et al. (2014). The computational box is $L = 2 \text{ kpc}$ on a side, and a maximum refinement level $l_{max} = 11$ is adopted, which corresponds to a minimum cell size of $\Delta x_{min} = 0.95 \text{ pc}$. The refinement strategy is geometry- and discontinuity-based. In particular, at each time step a number of cells at the highest refinement level is set up to cover the regions occupied by the OBAs. This assures that the OBAs are adequately spatially resolved (see next section). We use free outflow boundary conditions and create a passive scalar to trace the evolution of the metallicity of the gas in each cell, starting from a primordial value.

5. Results

Our main results can be summarized as follows.

- In the adiabatic case, the effects of feedback are to be regarded as maximal as, in principle, the energy injected by OBAs is entirely used to heat the interstellar medium. However, we find that the energy injected by the stars is not fully coupled to

the cold gas present in the system. After 30 Myr, the system has lost less than 20-30% of its initial gaseous mass (the exact figure depends on the location of the OBAs inside the simulation volume).

- The radiative high-resolution run was only followed for 20 Myr, for computational reasons. In this case, the cold, initial gas is even less affected by stellar feedback (Figs. 1 and 2).
- In both the adiabatic and radiative cases, a substantial amount of the hot ejecta provided by OBAs is lost from the system (Fig. 2). At the end of the simulations, the hot, metal-enriched tenuous gas driven by OBAs is not well-mixed with the cold, pristine gas.
- Interstellar bubbles are rapidly and efficiently created in both the adiabatic and radiative simulations (see Fig. 1, left and right panels, respectively). This occurs because of the high resolution of the simulations, which renders the effects of stellar feedback insensitive to the details of the subgrid physics (see also Read et al. 2016).
- From several convergence tests, and in agreement with other recent studies (Kim & Ostriker 2015; Martizzi et al. 2015; Simpson et al. 2015), we find that, if the cooling radius of the interstellar bubbles

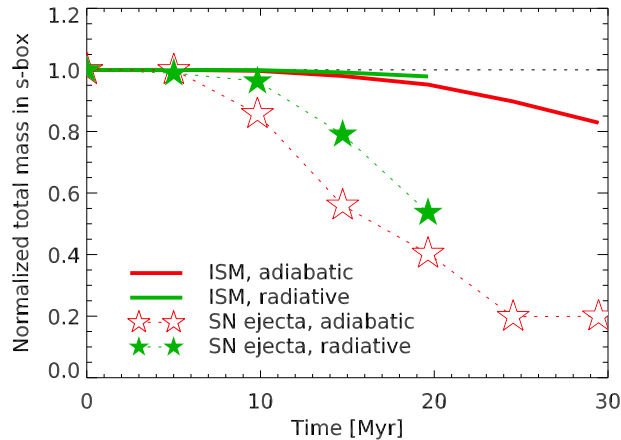


Fig. 2. Retained total gas (continuous lines) and metals (stars and dashed lines) in the simulation volume as a function of time, for the adiabatic (red) and radiative (green) highest-resolution simulations.

is resolved well enough, as it is in our high-resolution runs, the momentum that accompanies the fast ejecta of the OBA is correctly recovered before the deposited energy is radiated away.

Finally, it is important to note that there are well-known numerical difficulties in studies as the one described in this report. The fast fluid injected by stellar winds and SNe, with typical velocities of a few 10^3 km s $^{-1}$, is particularly difficult to treat computationally. This occurs mostly because, in order to satisfy the Courant-Friedrichs-Lowy condition, very small time steps are generally required. Some authors have chosen to overcome this difficulty by artificially decreasing the wind velocity (e.g. Emerick et al. 2019). In our simulations, the wind velocity has not been altered. We plan to investigate in more detail the consequences of different assumptions about the wind velocity on the chemical enrichment of small systems in future work.

6. Use of HPC resources and impact of research

As already mentioned, the HPC resources have been used to complete a set of high-resolution 3D simulations. This has lead to one publication on a peer-reviewed journal (Romano et al. 2019). Furthermore, the results have been

presented at conferences and workshops. The MoU INAF-CINECA has permitted a faster access to the necessary HPC resources and, hence, a faster publication.

References

- Bland-Hawthorn, J., et al. 2015, ApJ, 807, 154
- Brown, T. M., et al. 2014, ApJ, 796, 91
- Burkert, A. 1995, ApJ, 447, L25
- Corlies, L., et al. 2018, MNRAS, 475, 4868
- Emerick, A., et al. 2016, ApJ, 826, 148
- Emerick, A., et al. 2019, MNRAS, 482, 1304
- Jeon, M., et al. 2017, ApJ, 848, 85
- Kim, C.-G., Ostriker, E. C. 2015, ApJ, 802, 99
- Kroupa, P. 2001, MNRAS, 322, 231
- Leitherer, C., et al. 2014, ApJS, 212, 14
- Martizzi, D., et al. 2015, MNRAS, 450, 504
- Okamoto, S., et al. 2012, ApJ, 744, 96
- Plummer, H. C. 1911, MNRAS, 71, 460
- Read, J. I., et al. 2016, MNRAS, 459, 2573
- Romano, D., et al. 2015, MNRAS, 446, 4220
- Romano, D., et al. 2019, A&A, 630, A140
- Salvadori, S., Ferrara, A. 2009, MNRAS, 395, L6
- Simon, J. D. 2019, ARA&A, 57, 375
- Simpson, C. M., et al. 2015, ApJ, 809, 69
- Sutherland, R. S. 2010, Ap&SS, 327, 173
- Teyssier, R. 2002, A&A, 385, 337
- Vincenzo, F., et al. 2014, MNRAS, 441, 2815
- Webster, D., et al. 2015, ApJ, 799, L21